Solvent Effects on Ultraviolet Absorption and Circular Dichroic Spectra of Helical Polypeptides and Globular Proteins. Calculations Based on a Lattice-Filled Cavity Model

Jon Applequist* and Kimberly A. Bode

Department of Biochemistry, Biophysics, and Molecular Biology, Iowa State University, Ames, Iowa 50011

Received: October 27, 1998; In Final Form: January 11, 1999

Solvent effects on the electronic absorption and circular dichroic spectra of helical polypeptides and globular proteins are modeled by placing the molecule in a spherical cavity in a continuous dielectric medium and filling voids in the cavity with a simple cubic lattice of solvent molecules. Effects on the amide $\pi-\pi^*$ spectra near 200 nm are treated. The interactions among the solute atoms, solute chromophores, and discrete solvent molecules are treated by the partially dispersive dipole interaction treatment applied previously to the isolated molecules, while the dielectric continuum is treated by a rigorous reaction field formalism. Calculations are given for helical polypeptides α_R-$(Ala)_{10}$, $(Pro)_{10}$ II, β_P-$(Abu)_{6\times3}$, β_A-$(Abu)_{6\times3}$ and globular proteins erabutoxin, cytochrome *c*, and myoglobin. Predicted solvent effects are generally small, but include potentially measurable increases in intensities of CD bands in α_R-$(Ala)_{10}$, $(Pro)_{10}$ II, and the three proteins, and hypochromic shifts in the absorption bands of β-sheets.

Introduction

An understanding of the effects of solvent on electronic absorption and circular dichroic (CD) spectra of polypeptides and proteins is important for two reasons: (i) the solution spectra are commonly used to gain information on conformations and changes in conformation with solution conditions; and (ii) most theoretical work on the origins of these spectra has treated only the isolated molecule, ignoring possible effects from the surrounding solvent.

In recent studies[1−3] we have found that a dipole interaction model for the isolated molecule gives realistic predictions of absorption and CD spectra of a variety of helical polypeptides and globular proteins in the region of the amide $\pi-\pi^*$ transition centered around 200 nm. The results have shown that the nonchromophoric parts of the molecule have large effects on the spectra, raising the question of whether surrounding solvent would have effects of similar magnitude. The purpose of this paper is to apply the same model to these systems in which the solvent is included. We use a lattice-filled cavity model,[4,5] which treats the interactions among all polarizable units in the system, including solute atoms, solute chromophoric groups, solvent molecules, and surrounding dielectric, in a way that is consistent with the treatment of intramolecular interactions in the isolated molecule.

The problem of solvent effects was addressed earlier by Rabenold and Rhodes,[6] who used a cylindrical cavity model for the solvent environment of a long α-helix and a time-dependent Hartree treatment which reduces to the classical dipole interaction theory. In an approximation which neglects solvent−solvent interactions, they predicted substantial solvent effects on dipole strengths and rotational strengths of the exciton bands in the amide $\pi-\pi^*$ system. The present study is based on an improved treatment of the polypeptide chain itself and includes solute−solvent and solvent−solvent coupling to all orders. For the globular proteins we adopt realistic structures of the immediate solvent environment by incorporating water molecules present in the X-ray crystal structures. The predicted solvent effects on all molecules tend to be much smaller than those predicted by Rabenold and Rhodes.

Studies on the quantum mechanical theory of solvent effects on spectra up to 1994 have been reviewed by Tomasi and Persico.[7] Applications to known molecules in the past 10 years include the following. Blair et al.,[8] Luzhkov and Warshel,[9] and Broo et al.[10] used molecular mechanics/dynamics methods to model a solute molecule surrounded by a large number ($\sim10^2-10^3$) of water molecules and to predict electronic spectral shifts in formaldehyde,[8] conjugated organic molecules,[9] and uracil derivatives.[10] The continuum reaction field approach has been used by Karelson and Zerner,[11] Aguilar et al.,[12] Fox et al.,[13] Rivail et al.,[14] and Broo et al.[10] The methods were applied to electronic spectra of formamide,[12] pyrimidines,[10,11] and various organic dyes[11,13] and to the infrared spectrum of formaldehyde.[14] Some of these treatments include permanent dipole effects in polar solvents, while ours does not. On the other hand, none of these studies deals with solvent effects on CD spectra or with any system of chromophores as large as a protein molecule.

Each of the above methods has shown promise for particular purposes, though it seems fair to say that no one method stands out as clearly superior for all applications. We suggest that our lattice-filled cavity model is the best choice for the present study because of the following features. (i) It treats solute and nearby solvent by a consistent all-order dipole-interaction formalism combined with a rigorous treatment of the reaction field throughout the cavity. (ii) The interaction problem is solved completely in one sequence of matrix operations which require no iterations. (iii) Because of its reliance on polarizabilities of atoms and chromophoric groups instead of details of electronic states, the treatment is easily extended to much larger systems than can be treated accurately by quantum mechanical methods with available computers. (iv) The model has met a stringent test by reproducing the large observed solvent shifts in the frequency and oscillator strength in the visible absorption spectrum of β-carotene.[5]

10.1021/jp984233c CCC: $18.00
Published on Web 02/24/1999

Theory

The theory of our cavity model has been described in detail elsewhere,[4] and only a brief summary will be given here. Our system consists of an isotropic dielectric continuum in which is located a spherical cavity containing one solute molecule and a number of solvent molecules. The solute molecule is treated as an assembly of polarizable point particles (atoms and chromophoric groups) which interact with each other only by way of the fields of their induced dipole moments in the presence of an external field, giving due consideration to the cavity field and reaction field contributions to these fields. The formalism is that of classical electromagnetic theory. The solvent molecules within the cavity are treated as isotropic points which interact with the solute molecule and with each other just as if they were part of the solute molecule. The refractive index of the solvent and the polarizabilities of all nonchromophoric atoms are taken to be independent of wavenumber (nondispersive), while the NC′O chromophores are assigned a Lorentzian wavenumber dependence. The partially dispersive normal mode method[15] solves the interaction problem in terms of the normal modes of the full system of dipole oscillators, the number of normal modes being equal to the number of dispersive polarizabilities (chromophores) in the system. The quantities of primary interest are the molar absorption coefficient ϵ and the circular dichroism $\Delta\epsilon$, both on a residue-molar basis, in a medium of refractive index n (or optical dielectric constant n^2). These are given by[4,15,16]

$$\epsilon = \left(\frac{3n}{2n^2+1}\right)\frac{8\pi^2\bar{\nu}^2 N_A \Gamma}{6909 N_r}\sum_{k=1}^{q}\frac{D_k}{(\bar{\nu}_k^2-\bar{\nu}^2)^2+\Gamma^2\bar{\nu}^2} \quad (1)$$

$$\Delta\epsilon = \left(\frac{5n^2+1}{4n^2+2}\right)\frac{32\pi^3\bar{\nu}^3 N_A \Gamma}{6909 N_r}\sum_{k=1}^{q}\frac{R_k}{(\bar{\nu}_k^2-\bar{\nu}^2)^2+\Gamma^2\bar{\nu}^2} \quad (2)$$

where $\bar{\nu}$ is the wavenumber of the light, N_A is Avogadro's number, Γ is the half-peak bandwidth of all normal modes, q is the number of normal modes, N_r is the number of residues in the solute molecule, and $\bar{\nu}_k$, D_k, and R_k are the resonance wavenumber, dipole strength, and rotational strength of the kth normal mode.

The refractive index factors in eqs 1 and 2 are peculiar to the cavity model, and they convey only the effect of the medium on the fields of the light wave within the cavity. The equations show that these factors affect the overall intensity of the spectra, but not the band shape. Further effects of the medium are present by way of the reaction fields and the polarization of solvent molecules within the cavity. These effects are propagated through the normal mode moments and wavenumbers and affect the band shape through the relative intensities and splittings of the various normal modes.

Further quantities of interest are the mean absorption wavelength $\langle\lambda\rangle$ (approximately the peak wavelength), mean oscillator strength per residue $\bar{f}$, and total rotational strength per residue R'_{tot} (a measure of nonconservative rotational behavior), given by

$$\langle\lambda\rangle = [\sum_{k=1}^{q}\bar{\nu}_k^2 D_k/\sum_{k=1}^{q}D_k]^{-1/2} \quad (3)$$

$$\bar{f} = \left(\frac{3n}{2n^2+1}\right)(4m_e\pi^2c^2/3e^2N_r)\sum_{k=1}^{q}D_k \quad (4)$$

$$R'_{tot} = \left(\frac{5n^2+1}{4n^2+2}\right)(\pi hc/2N_r)\sum_{k=1}^{q}R_k \quad (5)$$

where m_e and e are the electron mass and charge, c is the vacuum velocity of light, and h is Planck's constant. The refractive index factors in eqs 4 and 5 are those which occur in the absorption and CD spectra, respectively, and which would therefore be present in oscillator strengths and rotational strengths obtained by integration of spectral bands. The factor $\pi hc/2$ in eq 5 converts our normal mode rotational strengths R_k to the conventional units in terms of electric and magnetic transition moments.[15] Numerically this factor is 3.365×10^{22} debye·bohr magnetons/cm^2.

For the helical structures we are also interested in the spectral components which are polarized parallel or perpendicular to the helix axis. For these cases we calculate the splitting Δ between the parallel and perpendicular absorption peaks and the parallel and perpendicular oscillator strengths per residue f and $f_\perp$ by

$$\Delta = [\sum_{k=1}^{q}\bar{\nu}_k^2 D_{k\perp}/\sum_{k=1}^{q}D_{k\perp}]^{1/2} - [\sum_{k=1}^{q}\bar{\nu}_k^2 D_{k\parallel}/\sum_{k=1}^{q}D_{k\parallel}]^{1/2} \quad (6)$$

$$f_\parallel = \left(\frac{3n}{2n^2+1}\right)(4m_e\pi^2c^2/3e^2N_r)\sum_{k=1}^{q}D_{k\parallel} \quad (7)$$

$$f_\perp = \left(\frac{3n}{2n^2+1}\right)(4m_e\pi^2c^2/3e^2N_r)\sum_{k=1}^{q}D_{k\perp} \quad (8)$$

Methods

The structures of regular polypeptide helices and sheets were generated as described previously.[17−20] Structures of erabutoxin, cytochrome *c*, and myoglobin were generated from X-ray crystal structures by the reassembled-fragment method described elsewhere.[3] In these proteins 10−15% of the residues were excluded to eliminate artifactual close contacts resulting from the method of reassembly, and a number of amino acid substitutions were made in order to limit the atoms to those with known polarizabilities and to reduce the conformational degrees of freedom in the side chains. Otherwise, all nonchromophoric atoms of the protein chain were included in the model and all NC′O groups were represented by a single point with an anisotropic core polarizability and a complex dispersive polarizability corresponding to the low energy $\pi-\pi^*$ transition. Atom polarizabilities were those used in our recent related calculations, namely (in Å^3): C, 0.777; H(alkane), 0.172; H(amide), 0.149.[21] Amide NC′O polarizabilities were those of parameter set H_y for all molecules except poly(proline), for which set J_y was used.[1]

For the cavity calculations the solute molecule was placed in a spherical cavity having a radius exceeding the circumsphere radius of the solute by the amount EXT. The circumsphere was determined using a program by Felder,[22] and the center of that sphere was taken as the cavity center. The voids in the cavity surrounding the solute were filled with isotropically polarizable points on a simple cubic lattice with spacing d. Any lattice point was excluded if it fell within a minimum contact distance CMOL of a solute point or within a minimum contact distance CWAL of the cavity wall. The polarizability α_L of each lattice point was taken in accordance with the Lorentz−Lorenz relation, $\alpha_L = (3d^3/4\pi)(n^2-1)/(n^2+2)$, so that an infinite lattice of the same structure would have the same refractive index n as the continuum.

TABLE 1. Cavity Size and Contents

molecule	circumsphere radius (Å)	cavity radius (Å)	bound waters	lattice points	residues
α_R-(Ala)$_{10}$	8.5	11.5	0	107	10
(Pro)$_{10}$ II	16.4	19.4	0	837	10
β_P-(Abu)$_{6\times3}$	11.3	14.3	0	206	18
β_A-(Abu)$_{6\times3}$	11.9	14.9	0	278	18
erabutoxin	22.9	23.9	99	1224	53
cytochrome *c*	21.2	22.2	121	602	88
myoglobin	25.7	26.7	110	1347	138

The computations were performed as described elsewhere.[3] The programs are available on the World Wide Web at http://www.public.iastate.edu/~jba/CaPPS. The most demanding computational steps are the solution to the eigenvalue problem of order q and the inversion of the nondispersive interaction matrix of order N_2. The largest system considered here is that of myoglobin + bound water in a filled cavity, for which $q = 138$ (the number of NC′O chromophores) and $N_2 = 8463$. The CPU time required for this system on a DEC 8400/440 workstation with 1 GB of memory and four parallel 440 MHz processors was about 1.5 h.

Results

Calculations are given here for the following molecules: (L-alanine)$_{10}$ in a right-handed α-helix, denoted α_R-(Ala)$_{10}$; (L-proline)$_{10}$ in a type II helix, or (Pro)$_{10}$ II; (L-α-aminobutyric acid)$_6$ in parallel and antiparallel β-sheets of three strands each, denoted β_P-(Abu)$_{6\times3}$ and β_A-(Abu)$_{6\times3}$, respectively; the β-type protein erabutoxin; and the α-type proteins cytochrome *c* and myoglobin. The half-peak bandwidth Γ is taken as 4000 cm^{-1} in all spectra shown here.

The CD spectra calculated for most of these molecules in the absence of solvent have been reported previously[1,3] and are reproduced here for comparison with the calculations based on the lattice-filled cavity model. Preliminary calculations of solvent effects for (Ala)$_{10}$ and (Pro)$_{10}$ have been presented.[23]

For the polypeptide helices and sheets the lattice parameters were EXT = CMOL = d = 3.0 Å and CWAL = 1.0 Å as justified previously.[4] The use of smaller values of EXT were attempted as a means of reducing the number of lattice points, but this was found to produce artifacts when $n^2 \geq 3$ due to the close proximity of a small number of solute atoms to the cavity wall. In exploratory calculations on (Pro)$_{10}$ II the results were found to be insensitive to CWAL over a range of 0.5−2.0 Å and insensitive to d over a range of 2.0−4.0 Å. The results were insensitive to CMOL in the range 3.0−5.0 Å, but were sensitive to this quantity at shorter distances; e.g., at CMOL ≤ 2.5 Å there were red shifts of 2−5 nm in both absorption and CD spectra. As such shifts are often artifacts resulting from close contacts, we regard them as unrealistic and report here only the results for CMOL = 3.0 Å, which is a typical nonbonded contact distance for small atoms.

For the proteins the solvent effects were calculated in two ways. (i) The water molecules found in the X-ray crystal structures were inserted into the structure as isotropic points at their original coordinates, and the system of protein + bound water was treated as an isolated molecule for comparison with calculations which omit the water. For erabutoxin 12 water molecules at low occupancy sites were deleted; in cytochrome *c* 3 waters were removed to eliminate close contacts, and in myoglobin 2 waters were removed for the same reason. (ii) The protein + bound water system was placed in a lattice-filled spherical cavity as described above, treating the waters of hydration as fixed parts of the solute. The lattice and surrounding continuum were taken to have the polarizability and refractive index of water at 200 nm and 20 °C, with $n^2 = 2.03$[24] and $\alpha_L = 1.83$ Å^3, and $d = 3.11$ Å from the molecular volume of 30.0 Å^3 for liquid water at 20 °C. As above, CMOL = 3.0 Å and CWAL = 1.0 Å, but EXT = 1.0 Å in order to minimize the number of lattice points. This choice for EXT is acceptable for use with the water parameters, as the results are essentially the same for erabutoxin in a larger cavity.

Table 1 shows the data on cavity size and cavity contents for the systems studied. Figures 1 and 2 show the structures of

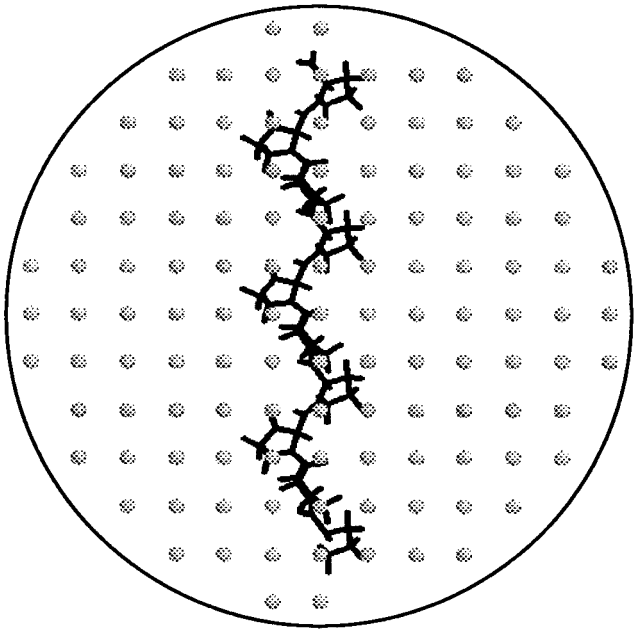

Figure 1. (Pro)$_{10}$ in the lattice-filled cavity. Small spheres represent solvent molecules. The lattice spacing is 3.0 Å. The space outside the large sphere is a continuous medium of refractive index n. Graphics by RasMol v2.6.

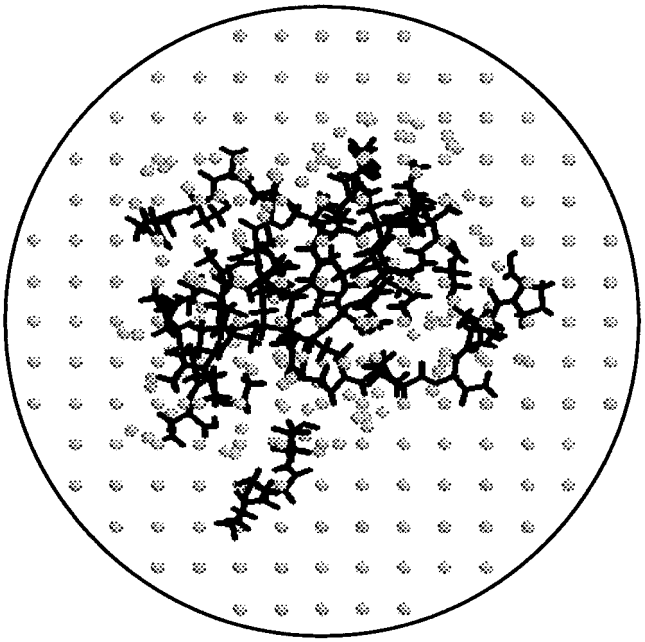

Figure 2. Erabutoxin in the lattice-filled cavity. Breaks in the protein chain show deletions made in the reassembly process. Small spheres represent both bound water molecules and surrounding solvent lattice. The lattice spacing is 3.11 Å. The space outside the large sphere is a continuous medium with the refractive index of water. Graphics by RasMol v2.6.

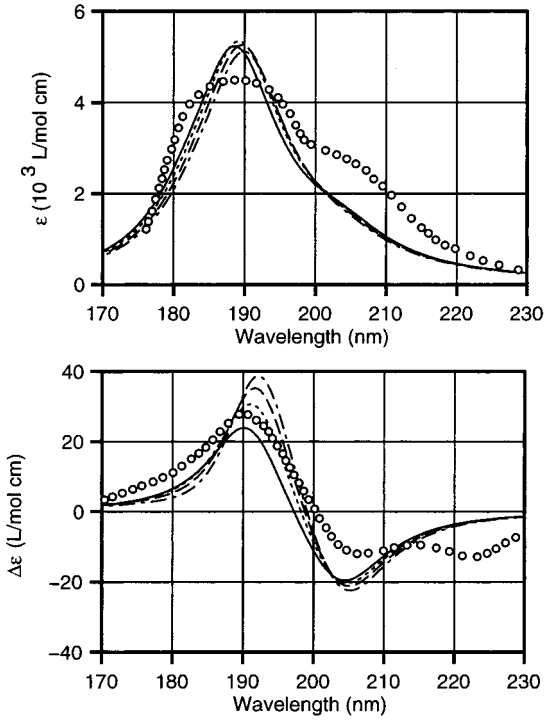

Figure 3. α_R-(Ala)$_{10}$ absorption and CD spectra in a lattice-filled spherical cavity: (—) $n^2 = 1.0$; (- - -) $n^2 = 2.0$; (— — —) $n^2 = 3.0$; (— · —) $n^2 = 4.0$. Experimental data (○) for poly(L-glutamic acid) in water from Tinoco et al.[28] (absorption, pH 4.9), and from Johnson and Tinoco[26] (CD, pH 4.5).

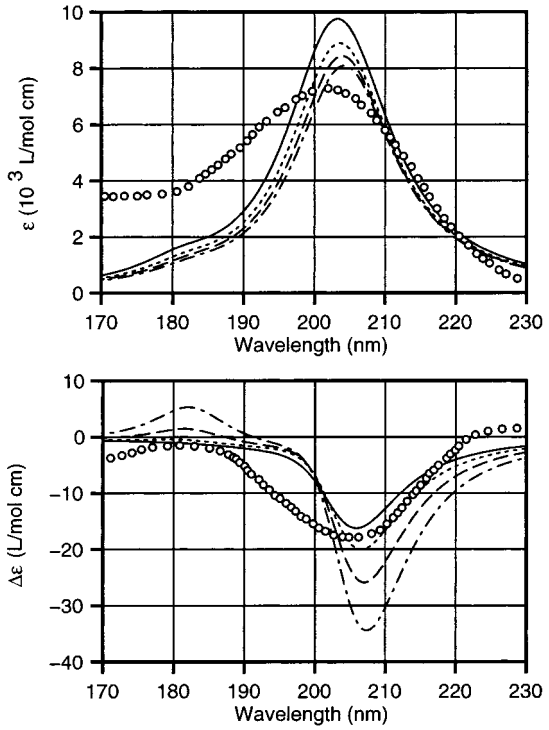

Figure 4. (Pro)$_{10}$ II absorption and CD spectra in a lattice-filled spherical cavity. Side chain torsion angle $\chi^2 = +20°$. (—) $n^2 = 1.0$; (- - -) $n^2 = 2.0$; (— — —) $n^2 = 3.0$; (— · —) $n^2 = 4.0$. Experimental data (○) for poly(l-proline) II in trifluoroethanol from Jenness et al.[29]

the cavity and contents for the (Pro)$_{10}$ II and erabutoxin molecules. The lattice structures show the placement of solvent molecules in the space not occupied by the solute, while the irregularly spaced solvent molecules in erabutoxin show bound water that is within and on the surface of the protein.

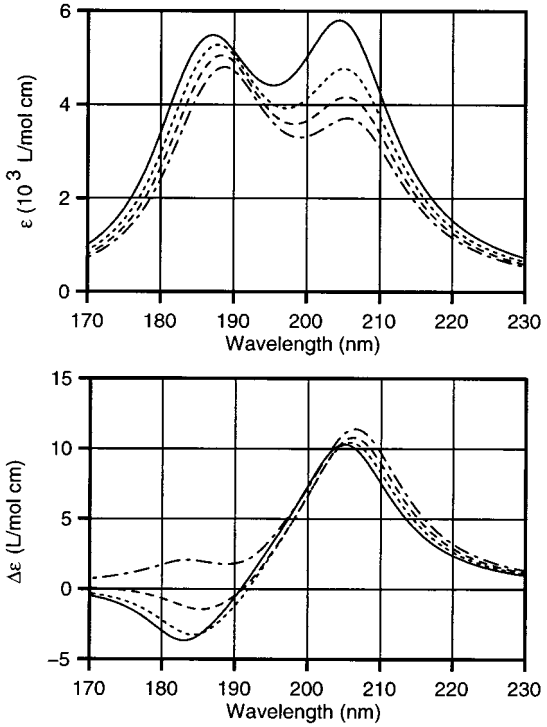

Figure 5. β_P-(Abu)$_{6\times3}$ absorption and CD spectra in a lattice-filled spherical cavity. Side chain torsion angle $\chi^1 = 180°$. (—) $n^2 = 1.0$; (- - -) $n^2 = 2.0$; (— — —) $n^2 = 3.0$; (— · —) $n^2 = 4.0$.

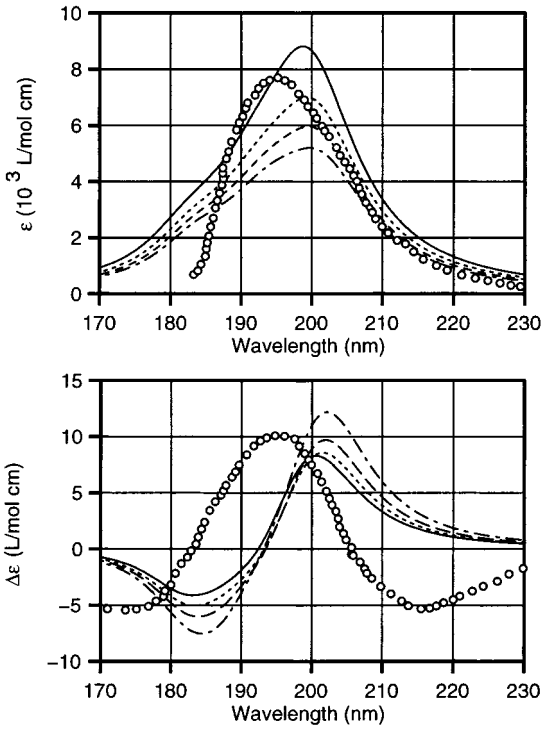

Figure 6. β_A-(Abu)$_{6\times3}$ absorption and CD spectra in a lattice-filled spherical cavity. Side chain torsion angle $\chi^1 = 180°$. (—) $n^2 = 1.0$; (- - -) $n^2 = 2.0$; (— — —) $n^2 = 3.0$; (— · —) $n^2 = 4.0$. Experimental data (○) for poly(L-lysine) in water from Rosenheck and Doty[30] (absorption, pH 10.8), and from Brahms et al.[31] (CD, pH 11.2).

Figures 3−6 show the calculated absorption and CD spectra for the helical polypeptides, including the β-sheets. The systems include the isolated molecule ($n^2 = 1$) and the lattice-filled cavity models with $n^2 = 2.0$, 3.0, 4.0. Table 2 summarizes the dependence of the main spectral features on n^2. There λ_{CD1} and λ_{CD2} are the peak wavelengths of the CD bands. Figures 7−9

TABLE 2. Spectral Properties of Helical Polypeptides at Various Values of n^2

molecule	property	$n^2 = 1$	$n^2 = 2$	$n^2 = 3$	$n^2 = 4$
α_R-(Ala)$_{10}$	$\langle\lambda\rangle$ (nm)	190	190	190	191
	$\bar{\Delta}$ (cm^{-1})	3113	2916	2777	2650
	$\bar{f}$	0.169	0.169	0.165	0.159
	$f_{\parallel}$	0.024	0.020	0.018	0.017
	$f_{\perp}$	0.145	0.149	0.146	0.142
	$f_{\parallel}/f_{\perp}$	0.164	0.136	0.124	0.117
	R'_{tot} (D·μ_B)	0.069	0.172	0.207	0.196
	λ_{CD1} (nm)	204	204	206	208
	λ_{CD2} (nm)	190	192	192	192
(Pro)$_{10}$ II[a]	$\langle\lambda\rangle$ (nm	202	203	203	203
	$\bar{\Delta}$ (cm^{-1})	907	807	775	767
	$\bar{f}$	0.290	0.259	0.243	0.231
	$f_{\parallel}$	0.114	0.073	0.056	0.047
	$f_{\perp}$	0.176	0.186	0.187	0.185
	$f_{\parallel}/f_{\perp}$	0.644	0.390	0.300	0.253
	R'_{tot} (D·μ_B)	−0.437	−0.487	−0.560	−0.642
	λ_{CD} (nm)	202	206	208	208
β_P-(Abu)$_{6\times3}$[b]	$\langle\lambda\rangle$ (nm)	195	195	195	195
	$\bar{\Delta}$ (cm^{-1})	4568	4490	4402	4312
	$\bar{f}$	0.281	0.250	0.229	0.212
	$f_{\parallel}$	0.145	0.117	0.100	0.088
	$f_{\perp}$	0.136	0.134	0.129	0.123
	$f_{\parallel}/f_{\perp}$	1.072	0.874	0.778	0.718
	R'_{tot} (D·μ_B)	0.191	0.202	0.259	0.371
	λ_{CD1} (nm)	204	206	206	206
	λ_{CD2} (nm)	184	184	186	
β_A-(Abu)$_{6\times3}$[b]	$\langle\lambda\rangle$ (nm)	196	196	196	196
	$\bar{\Delta}$ (cm^{-1})	2484	2594	2620	2616
	$\bar{f}$	0.303	0.252	0.222	0.198
	$f_{\parallel}$	0.210	0.160	0.132	0.113
	$f_{\perp}$	0.093	0.093	0.090	0.086
	$f_{\parallel}/f_{\perp}$	2.261	1.725	1.471	1.313
	R'_{tot} (D·μ_B)	0.078	0.059	0.062	0.092
	λ_{CD1} (nm)	200	202	202	202
	λ_{CD2} (nm)	184	184	184	184

[a] Side chain torsion angle $\chi^2 = 20°$. [b] Side chain torsion angle $\chi^1 = 180°$.

show the calculated spectra for erabutoxin, cytochrome *c*, and myoglobin for the isolated molecule, protein + bound water, and protein + bound water + lattice + surrounding continuum. Table 3 summarizes the main spectral features for each case.

Discussion

Possibly the most significant finding of this study is the small magnitude of the solvent effects on the absorption and CD spectra of the molecules studied. In the globular proteins, the intimately associated bound water molecules have very little effect on the spectra, indicating that the predicted effects come primarily from long-range interactions with the surrounding medium.

Potentially measurable effects include (i) increases in intensities of certain CD bands in the α-helix, the (Pro)$_n$ II helix, and the three globular proteins; and (ii) hypochromic shifts in the absorption spectra of the β-sheets and the β-type protein erabutoxin. Observing these effects would be experimentally difficult, as the maximum range of variation of n^2 for known solvents is of the order of ∼1. The largest predicted shifts over this range are of the order of 10−20%, and this would place a severe limit on the acceptable uncertainty of measurement. In addition, the solvents would have to support the same conformation of each molecule and would have to be transparent at 200 nm.

Smith and Woody[25] measured the CD spectrum of α-helical poly(γ-*n*-dodecyl-L-glutamate) in three hydrocarbon solvents with n_D^2 from 1.89 to 2.03. Their spectra showed no shift in

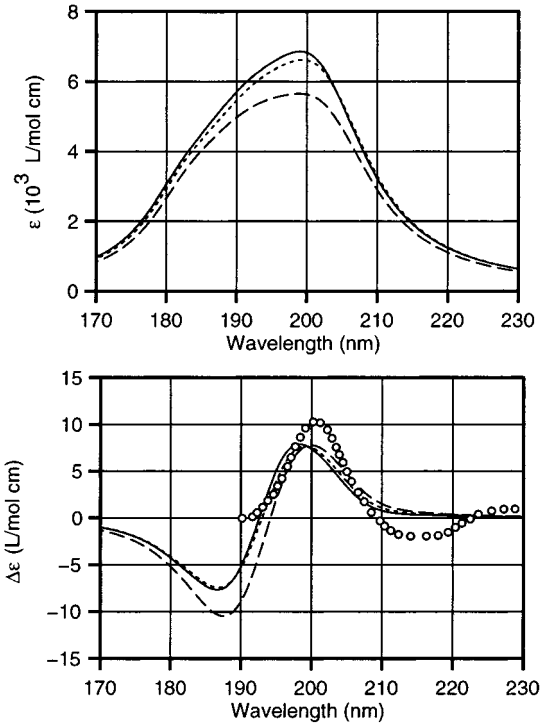

Figure 7. Erabutoxin absorption and CD spectra; (—) protein only; (- - -) protein + bound waters; (— — —) protein + bound waters + lattice + continuum. $n^2 = 2.03$. Experimental data (○) in 1 mM phosphate buffer at pH 6.5 from Dahms and Szabo.[32]

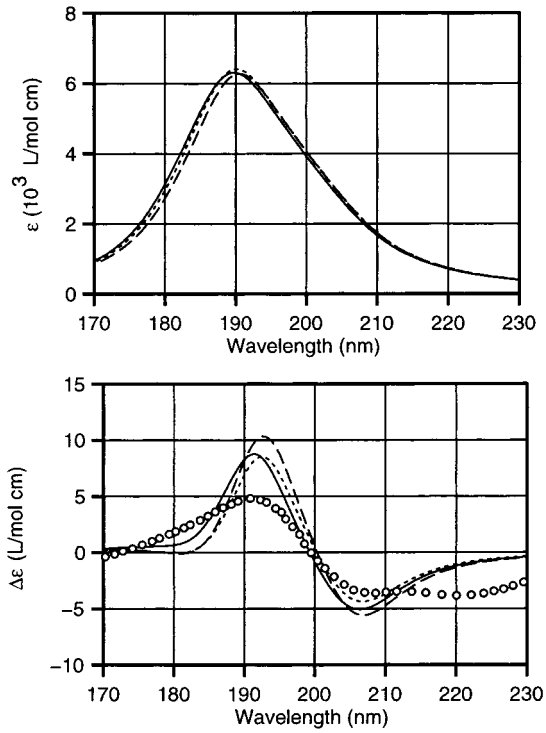

Figure 8. Cytochrome *c* absorption and CD spectra; (—) protein only; (- - -) protein + bound waters; (— — —) protein + bound waters + lattice + continuum. $n^2 = 2.03$. Experimental data (○) at neutral pD in 0.1 M NaF in D_2O from Brahms and Brahms.[33]

this range beyond the limits of error (∼10% at 190 nm), consistent with our calculations. A comparison of their CD spectra with that of Johnson and Tinoco[26] for α-helical poly(L-glutamic acid) in water (reproduced in Figure 3) shows nearly identical band intensities along with a blue shift of about 2 nm in water relative to hydrocarbon. This shift could arise from

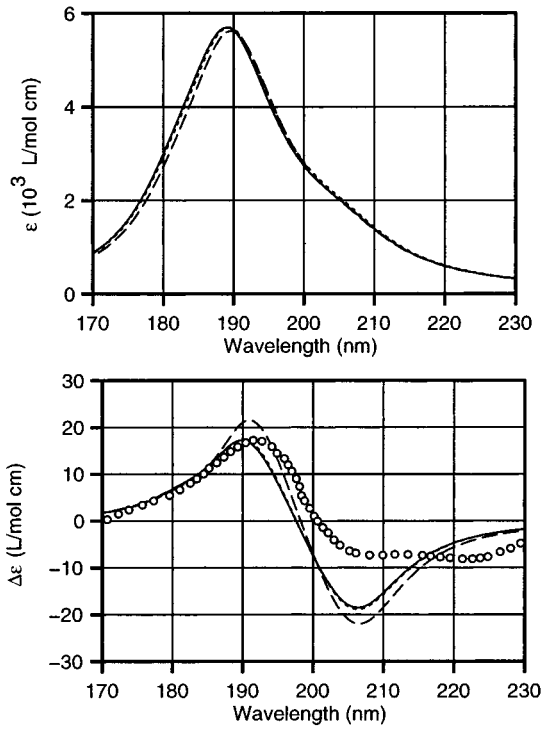

Figure 9. Myoglobin absorption and CD spectra. (—) protein only; (- - -) protein + bound waters; (— — —) protein + bound waters + lattice + continuum. $n^2 = 2.03$. Experimental data (○) in 0.01 M sodium phosphate buffer at pH 6.8 from Hennessey and Johnson.[34]

TABLE 3. Spectral Properties of Globular Proteins with and without Aqueous Environments

protein	property	I[a]	II[b]	III[c]
erabutoxin	$\langle\lambda\rangle$ (nm)	195	195	195
	f	0.285	0.278	0.247
	R'_{tot} (D·μ_B)	−0.037	−0.033	−0.098
	λ_{CD1} (nm)	198	200	200
	λ_{CD2} (nm)	186	186	188
cytochrome *c*	$\langle\lambda\rangle$ (nm)	191	192	192
	f	0.233	0.233	0.226
	R'_{tot} (D·μ_B)	0.040	0.034	0.037
	λ_{CD1} (nm)	206	206	206
	λ_{CD2} (nm)	192	192	192
myoglobin	$\langle\lambda\rangle$ (nm)	190	190	191
	f	0.200	0.200	0.194
	R'_{tot} (D·μ_B)	−0.026	−0.036	−0.025
	λ_{CD1} (nm)	206	206	206
	λ_{CD2} (nm)	190	190	190

[a] Protein only. [b] Protein + bound waters. [c] Protein + bound waters + lattice + continuum.

electrostatic interaction of the polar solvent with the chromophores,[7] an effect not considered in our model. Alternatively, small variations in the helical structure could produce shifts of this magnitude according to our predictions for helices occurring in globular proteins[3]. However, the small magnitude of the blue shift helps to justify the neglect of solvent polarity in our model.

Our predictions for the α-helix differ substantially from the earlier results of Rabenold and Rhodes.[6] Using parameters for water as solvent, they predict a 23.6% increase in $f_\perp$ and a 47% decrease in $f_\parallel$ due to the presence of water. Our data in Table 2 indicate only a 2.8% increase in $f_\perp$ and a 17% decrease in $f_\parallel$ at $n^2 = 2.0$, approximately the value for water. They predict a 12% decrease in the rotational strengths of the two CD bands due to solvent. While we do not separate the total rotational strength into two bands, it is evident from Figure 3 that the calculations show an *increase* of ∼30% in the 192 nm peak and little change in the negative peak at 204 nm. As Rabenold and Rhodes pointed out, their neglect of solvent−solvent coupling would have an effect on their results. Our calculations include solvent−solvent coupling to all orders, and this is probably the main reason for the discrepancies.

A particularly surprising result of these calculations is the extreme insensitivity of the splitting Δ to solvent for the helical polypeptides (Table 2). A view taken by some workers in past years is that the chromophores are bathed in a dielectric continuum which approximates the effects of all polarizable material in the environment, including solvent. If this view were valid, a large solvent effect on Δ would be expected; i.e., pairwise interaction energies would vary as $1/n^2$, and the first-order splitting[27] would vary in the same way. Our results show a much smaller effect than this; in fact Δ decreases with increasing n^2 in only three cases, while for the β_A-sheet the reverse is found. In our model the main effects of the polarizable environment come from the nonchromophoric atoms in the solute molecule itself. A similar conclusion was reached in an application of the same model to the spectra of the small peptide cyclo(Ala-Ala).[4]

Finally, it is worth noting that the present results justify the use of calculations for an isolated molecule as an approximation to the electronic absorption and CD spectra of polypeptides and proteins in solution. Our findings indicate cases where small discrepancies between experimental spectra and isolated-molecule theory might be attributable to solvent effects, but at present neither theory nor experiment is accurate enough to make such interpretations.

References and Notes

(1) Bode, K. A.; Applequist, J. *J. Phys. Chem.* **1996**, *100*, 17825. Erratum *J. Phys. Chem. A* **1997**, *101*, 9560.
(2) Bode, K. A.; Applequist, J. *Biopolymers* **1997**, *42*, 855.
(3) Bode, K. A.; Applequist, J. *J. Am. Chem. Soc.* **1998**, *120*, 10938. Erratum, *J. Am. Chem. Soc.* **1998**, *120*, 13545.
(4) Applequist, J. *J. Phys. Chem.* **1990**, *94*, 6564.
(5) Applequist, J. *J. Phys. Chem.* **1991**, *95*, 3539.
(6) Rabenold, D. A.; Rhodes, W. *J. Chem. Phys.* **1984**, *80*, 3866.
(7) Tomasi, J.; Persico, M. *Chem. Rev.* **1994**, *94*, 2027.
(8) Blair, J. T.; Krogh-Jespersen, K.; Levy, R. M. *J. Am. Chem. Soc.* **1989**, *111*, 6948.
(9) Luzhkov, V.; Warshel, A. *J. Am. Chem. Soc.* **1991**, *113*, 4491.
(10) Broo, A.; Pearl, G.; Zerner, M. C. *J. Phys. Chem. A* **1997**, *101*, 2478.
(11) Karelson, M. M.; Zerner, M. C. *J. Phys. Chem.* **1992**, *96*, 6949.
(12) Aguilar, M. A.; Olivares del Valle, F. J.; Tomasi, J. *J. Chem. Phys.* **1993**, *98*, 7375.
(13) Fox, T.; Rösch, N.; Zauhar, R. J. *J. Comput. Chem.* **1993**, *14*, 253.
(14) Rivail, J.; Rinaldi, D.; Dillet, V. *Mol. Phys.* **1996**, *89*, 1521.
(15) Applequist, J.; Sundberg, K. R.; Olson, M. L.; Weiss, L. C. *J. Chem. Phys.* **1979**, *70*, 1240. Erratum, *J. Chem. Phys.* **1979**, *71*, 2330.
(16) Applequist, J. *J. Chem. Phys.* **1979**, *71*, 1983.
(17) Applequist, J. *Biopolymers* **1981**, *20*, 387.
(18) Applequist, J. *Biopolymers* **1981**, *20*, 2311.
(19) Applequist, J. *Biopolymers* **1982**, *21*, 779.
(20) Thomasson, K. A.; Applequist, J. *Biopolymers* **1991**, *31*, 529.
(21) Bode, K. A.; Applequist, J. *J. Phys. Chem.* **1996**, *100*, 17820.
(22) Felder, C. E. Ph.D. Thesis, Iowa State University, Ames, Iowa, 1981.
(23) Applequist, J. *Chirality and Circular Dichroism: Structure Determination and Analytical Applications*; 5th International Conference on Circular Dichroism; Colorado State University: Fort Collins, CO, 1993; pp 152−157.
(24) Dorsey, N. E. *Properties of Ordinary Water-Substance*; ACS Monograph; Hafner Publishing Co., New York, 1968; p 283.
(25) Smith, J. C.; Woody, R. W. *Biopolymers* **1973**, *12*, 2657.
(26) Johnson, Jr., W. C.; Tinoco, Jr., I. *J. Am. Chem. Soc.* **1972**, *94*, 4389.
(27) Moffitt, W. *J. Chem. Phys.* **1956**, *25*, 467.
(28) Tinoco, Jr., I.; Halpern, A.; Simpson, W. T. In *Polyamino Acids, Polypeptides, and Proteins*, Stahmann, M. A., Ed.; University of Wisconsin Press: Madison, WI, 1962; Chapter 13, pp 147−157.
(29) Jenness, D. D.; Sprecher, C.; Johnson, Jr., W. C. *Biopolymers* **1976**, *15*, 513.

(30) Rosenheck, K.; Doty, P. *Proc. Natl. Acad. Sci. U.S.A.* **1961**, *47*, 1775.
(31) Brahms, S.; Brahms, J.; Spach, G.; Brack, A. *Proc. Natl. Acad. Sci. U.S.A.* **1977**, *74*, 3208.
(32) Dahms, T. E.; Szabo, A. G. *Biophys. J.* **1995**, *69*, 569.
(33) Brahms, S.; Brahms, J. *J. Mol. Biol.* **1980**, *138*, 149.
(34) Hennessey, Jr., J. P.; Johnson, Jr., W. C. *Biochemistry* **1981**, *20*, 1085.